Helicobacter

WILEY

Helicobacter

ORIGINAL ARTICLE OPEN ACCESS

Proteomic Profiling of Extracellular Vesicles Reveals Potential Biomarkers for *Helicobacter pylori* Infection and Gastric Cancer

Phawinee Subsomwong[1,2] | Krisana Asano[1] | Junko Akada[2] | Takashi Matsumoto[2,3] | Akio Nakane[1,4] | Yoshio Yamaoka[2,3,5]

[1]Department of Microbiology and Immunology, Hirosaki University Graduate School of Medicine, Hirosaki, Japan | [2]Department of Environmental and Preventive Medicine, Faculty of Medicine, Oita University, Yufu, Japan | [3]Research Center for Global and Local Infectious Diseases, Oita University, Yufu, Japan | [4]Department of Biopolymer and Health Science, Hirosaki University Graduate School of Medicine, Hirosaki, Japan | [5]Department of Medicine, Gastroenterology and Hepatology Section, Baylor College of Medicine, Houston, Texas, USA

Correspondence: Phawinee Subsomwong (phawinee@hirosaki-u.ac.jp; pha_203@hotmail.com) | Yoshio Yamaoka (yyamaoka@oita-u.ac.jp)

Received: 14 November 2024 | **Revised:** 4 February 2025 | **Accepted:** 13 February 2025

Funding: This study was supported by the Research Center for GLOBAL and LOCAL Infectious Diseases, Oita University (Grant Number 2021B12, 2021–2024), Japan Society for the Promotion of Science KAKENHI (Grant Number 22K15454, 2022–2024, 23K06525, 2023–2025), and the Research Grant from Ichimaru Pharcos Co. Ltd. (Grant Number 531021K019, 2023).

Keywords: biomarker | extracellular vesicles | gastric cancer | *Helicobacter pylori* | proteomics

ABSTRACT

Background: *Helicobacter pylori* (*H. pylori*) has been identified as a type I carcinogen and contributes to a high rate of gastric cancer (GC), especially in Eastern Asia. Extracellular vesicles (EVs) have the potential to be used to detect various cancer types and diseases. However, the protein markers in EVs for the prognosis of *H. pylori* infection and GC are unknown. We aim to identify the proteins within EVs derived from a gastric epithelial cell line (AGS) infected with *H. pylori* by using LC-MS/MS.

Materials and Methods: EVs were isolated from AGS cells infected with high- and low-virulence *H. pylori* (strains TN2wt and Tx30a) by ultracentrifugation. Proteins within these EVs were identified and analyzed for potential marker candidates through bioinformatics. Proteins in *H. pylori*-derived EVs (HpEVs) from bacterial culture supernatant and HpEVs derived from *H. pylori*-infected AGS cells were elucidated.

Results: Differentially expressed proteins by proteomic analysis in AGSEVs-Tx30a vs. AGSEVs-noninfected (NI) and AGSEVs-TN2wt vs. AGSEVs-NI were 107 and 55 proteins, respectively. Bioinformatics of these proteomes revealed that essential proteins for *H. pylori* survival and pathogenicity including outer membrane proteins, metabolism-related, host cell infection-related, and virulence-related proteins were observed in HpEVs. Interestingly, EVs derived from AGS cells infected with *H. pylori* TN2wt significantly contained multiple proteins related to GC (ATP6V0A1, GAPDH, HINT1, LYZ, and RBX1).

Conclusion: This study provides a comprehensive protein profile of EVs from *H. pylori*-infected AGS cells and HpEVs, which could serve as liquid-based biomarkers in the future for screening *H. pylori* infection, especially GC-related.

1 | Introduction

Helicobacter pylori (*H. pylori*) is a Gram-negative spiral bacterium that persists in the stomach of nearly half of the global population [1]. It causes several gastrointestinal diseases, including chronic gastritis, peptic ulcer, gastric mucosa-associated lymphoid tissue lymphoma, and gastric cancer (GC) [2, 3]. The GLOBOCAN 2022 database on cancer incidence

and mortality reported that *H. pylori* is the primary infectious agent responsible for gastric cancer (968,000 cases, with an age-standardized incidence rate of 9.2 cases per 100,000 person-years) [4].

H. pylori virulence factors are associated with the severity of disease and long-term patient outcomes [5]. Individuals infected with *cagA*-positive *H. pylori* have an increased risk of peptic ulcer disease, atrophic gastritis, intestinal metaplasia, and GC compared to those infected with *cagA*-negative strains [6, 7]. The vacuolating ability differs depending on the *vacA* genotype. The *vacA* s1m1 type strain produces vacuolating toxin and is more likely to be associated with GC than the s2m2 type, which is a non-vacuolating type [8, 9]. Other virulence factors such as blood group antigen binding adhesion (BabA) and sialic acid binding adhesin (SabA) are involved in the colonization and persistence of *H. pylori* in the stomach [10]. The outer inflammatory protein A (OipA), duodenal ulcer promoting (DupA), and induced by contact with epithelium (IceA) contribute to promoting inflammation, tissue damage, and clinical development [11–13]. *H. pylori*-positive for these virulence factors tend to cause more severe outcomes compared to strains lacking them.

Extracellular vesicles (EVs) are membrane-enclosed structures that contain a variety of biologically active molecules, including proteins, lipids, and nucleic acids. EVs can be classified into several types based on their size: microvesicles (100–1000 nm), exosomes (30–150 nm), and apoptotic bodies (800–5000 nm). They are derived from their originating cells, and they have been found in various body fluids, such as blood, saliva, urine, and excrement [14, 15]. The biologically active molecules encapsulated within the EVs are protected from degradation and have the potential to be used as a non-invasive biomarker [16, 17]. *H. pylori*-derived EVs (HpEVs) are nanosized particles of approximately 20 to 450 nm. They are obtained from the outer membrane of *H. pylori* and retain many surface molecules, including lipopolysaccharide, peptidoglycan, and outer membrane proteins [18, 19]. The virulence-related proteins such as urease subunit, VacA, CagA, γ-glutamyl transpeptidase, and cytoplasmic proteins GroEL were identified in HpEVs [19].

Blood-based biomarkers have been developed to minimize invasive techniques, particularly in diagnosing cancers and pathogen infections. It has been shown that EVs are secreted by tumors into the bloodstream and carry various functional proteins [20, 21]. EV-bound proteins have been used as biomarkers for monitoring, predicting, and detecting several cancers, including breast, lung, colorectal, pancreatic, and prostate, etc. [22–24]. The expression of CD91 in lung cancer cells and circulating EVs in blood serves as a potential biomarker of non-small cell lung cancer patients [25]. Likewise, the increase of CD147 in EVs could be used as a non-invasive marker for the diagnosis and prognosis of colorectal cancer [26]. Many studies use the contents in the EVs released from bacteria to diagnose infectious diseases. EVs derived from *Pseudomonas aeruginosa* containing cystic fibrosis transmembrane conductance regulator inhibitory factor were used to diagnose cystic fibrosis [27]. A 19 kDa lipoprotein, Lpqh, found in the cell wall of *Mycobacterium tuberculosis* was used as the plasma biomarker to distinguish between paratuberculosis and tuberculosis infection in cows [28]. Therefore, a blood-based biomarker is useful for screening the markers of both cancers and infections.

In this study, we used liquid chromatography–tandem mass spectrometry (LC–MS/MS) to identify the proteins within EVs derived from a gastric cell line infected with high- and low-virulence strains of *H. pylori*. In addition, we investigated the differential proteins that have the potential to serve as candidate protein markers for the prognosis of GC and *H. pylori* infection. Furthermore, we identified proteins in HpEVs and *H. pylori* secreted during gastric cell line infection. We expect that our results could provide candidate protein markers for detecting virulent *H. pylori* infections in body fluids, offering a more convenient screening method in the future.

2 | Materials and Methods

2.1 | Bacterial Strains and Culture Conditions

H. pylori strain TN2wt and *H. pylori* strain Tx30a were subcultured on trypticase soy agar (TSA) with 5% (v/v) sheep's blood (Nissui Pharmaceutical Co. Ltd., Tokyo, Japan) and incubated in a sealed jar (Mitsubishi Gas Chemical Co. Inc., Tokyo, Japan) under a microaerophilic atmosphere (AnaeroPac- MicroAero; Mitsubishi Gas Chemical Co. Inc.) at 37°C for 48 h.

2.2 | Cell Line and Culture Conditions

Human adenocarcinoma gastric epithelial cell line (AGS) was obtained from the Department of Environmental and Medicine, Faculty of Medicine, Oita University, Oita, Japan. The cells were cultured in RPMI 1640 (Nissui Pharmaceutical Co. Ltd) supplemented with 10% heat-inactivated fetal bovine serum (FBS; JRH Biosciences, Lenexa, Kansas), 0.03% L-glutamine (Wako Pure Chemical Industries, Osaka, Japan), and 1× antibiotic-antimycotic (Gibco; ThermoFisher Scientific, Waltham, MA, USA) and incubated under 5% CO_2 at 37°C for 48 h.

2.3 | Cytotoxic Effect of AGS Cells With *H. pylori*

The cytotoxicity effect of *H. pylori* on AGS cells was performed in 96-well plates. AGS cells (2×10^4 cells/well) were seeded in the plate and incubated under 5% CO_2 at 37°C for 48 h. The cells were washed with phosphate-buffered saline (PBS) three times for 5 min before *H. pylori* infection. The *H. pylori* strains were suspended in RPMI medium without FBS and antibiotic-antimycotic, and the bacterial count was adjusted based on optical density at OD 600 nm (OD_{600nm}) using a spectrophotometer (OD_{600nm} of 1.0 corresponds to 3.3×10^8 CFU/mL and 4.6×10^8 CFU/mL for *H. pylori* Tx30a and TN2wt). The AGS cells were infected with *H. pylori* Tx30a or TN2wt strains at a multiplicity of infection (MOI) = 100 and incubated under 5% CO_2 at 37°C for 48 h. The cell viability was assessed using a WST-1 cell proliferation kit (Roche Diagnostic, Mannheim, Germany) as described in the manufacturer's instructions. Briefly, 10 μL of WST-1 reagent was added directly into the well and incubated at 5% CO_2 at 37°C until color development. The absorbance at 450 nm and 600 nm was measured using a microplate reader

(MULTISKAN Sky, Thermo Fisher Scientific). The absorbance values were subtracted from the cell-free medium, and the viability of AGS cells without *H. pylori* infection was calculated as 100%.

2.4 | Infection of AGS Cells With *H. pylori*

The AGS cells (2×10^7 cells/flask) were seeded in a 75 cm^2 flask and incubated under 5% CO_2 at 37°C for 48 h. The cells were washed with 10 mL PBS for 5 min three times before *H. pylori* infection. The *H. pylori* strains were prepared as described above. The AGS cells were infected with *H. pylori* Tx30a or TN2wt strains at MOI = 100 and incubated at 5% CO_2 at 37°C for 48 h. The cell culture supernatant was collected for EV isolation.

2.5 | Isolation of EVs From AGS Cell Culture Supernatant

AGS cells, its cell debris, and *H. pylori* were removed from the cell culture supernatant by centrifugation at 2000×*g* for 30 min at 4°C, followed by filtration through a 0.45 μm filter (Nalgene Rapid-Flow Filters, Thermo Fisher Scientific). The EVs were collected by ultracentrifugation at 110,000×*g* for 70 min using Himac CP80NX Preparative Ultracentrifuge (HITACHI, Tokyo, Japan). After the removal of the supernatant, EVs were washed with PBS and then collected by ultracentrifugation at 100,000×*g* for 70 min at 4°C. Finally, the EVs were resuspended in 100 μL PBS and frozen at −80°C.

2.6 | Detection of AGS Cell-Derived EVs

EVs were detected by an immunoblotting assay. Briefly, the AGS cell-derived EVs were dot-blotted on the polyvinylidene difluoride membrane. The membrane was blocked with 5% skim milk in washing buffer (0.05% Tween 20 in PBS) and then incubated with the primary antibody against TSG101 (ab125011, dilution 1:1000, Abcam, UK) at 4°C overnight. After washing the membrane, the secondary antibody, horseradish peroxidase-conjugated Goat-anti-Rabbit IgG (MP Biomedicals, dilution 1:1000, Irvine, CA) was added and incubated at RT for 2 h, followed by washing three times SuperSignal West Dura chemiluminescence substrate (Thermo Scientific, IL) was used to detect the signal, and images were taken using Chemidoc XRS+ (Biorad, CA). The particles of AGS cell-derived EVs were confirmed under the transmission electron microscope (JEM-1230, JEOL, Tokyo, Japan) with negative staining (TI blue, Nisshin EM Co. Ltd., Tokyo, Japan).

2.7 | *H. pylori* Conditions for HpEVs Isolation

Culture conditions for *H. pylori* were modified as described previously [29]. Briefly, *H. pylori* strains (Tx30a and TN2wt) were suspended in Brucella broth (BB; BD Bioscience, Sparks, MD) supplemented with 5% exosomes-depleted fetal bovine serum (FBS) (Biosera, Cholet, France). The initial OD_{600nm} of the bacterial suspension was adjusted to 0.02 in 20 mL of BB + 5% exosomes-depleted FBS. The *H. pylori* strains were grown in a 50 mL flask, placed in a sealed jar under microaerophilic conditions, and shaken at 100 rpm at 37°C for 0 to 96 h. The growth curve of each strain of *H. pylori* was monitored by measuring OD_{600nm} and counting the number of viable bacterial numbers by plate count assay on TSA + 5% (v/v) sheep's blood (Nissui Pharmaceutical Co. Ltd.).

H. pylori cell viability was monitored using the LIVE/DEAD BacLight Bacterial Viability Kit (Invitrogen, Waltham, MA). Live cells were stained with SYTO9 (green fluorescence) and dead cells were stained with propidium iodide (red fluorescence). Fluorescence signals were observed under a fluorescence microscope (KEYENCE, BZ-X700, Osaka, Japan).

2.8 | Isolation of HpEVs From *H. pylori* Culture Supernatant

The conditions for culturing *H. pylori* and isolating the HpEVs were modified as described previously [29]. *H. pylori* strains were suspended in BB supplemented with 5% exosome-depleted FBS. The initial OD_{600nm} of the bacterial suspension was adjusted to 0.02 in 200 mL of BB + 5% exosome-depleted FBS. The *H. pylori* strains were grown in a 500 mL flask and placed in a sealed jar under microaerophilic conditions and shaking at 100 rpm at 37°C for 48 h. The *H. pylori* cells were removed from the culture supernatant by centrifugation at 15,000×*g* for 15 min at 4°C. The bacteria-free supernatant was filtered through a 0.45 μm filter and kept at −80°C until HpEVs isolation. HpEVs in the 400 mL of culture supernatant of *H. pylori* strains were harvested by ultracentrifugation at 200,000×*g* for 90 min at 4°C. After the removal of the supernatant, HpEVs were washed in 20 mL of 0.9% NaCl solution and then collected by ultracentrifugation at 200,000×*g* for 90 min at 4°C. HpEVs were resuspended in 200 μL saline and frozen at −80°C. The particles of HpEVs were confirmed under the transmission electron microscope with negative staining, as mentioned above.

2.9 | Proteomic Analysis of AGS Cell-Derived EVs and HpEVs

The protein concentration of the AGS cell-derived EVs were measured by the Bradford protein assay (Bio-Rad Laboratories, Richmond, CA). AGS cell-derived EVs were analyzed by LC–MS/MS as described in our previous study [30]. Briefly, EVs from three sample groups AGSEVs-NI, AGSEVs-Tx30a, and AGSEVs-TN2wt were lysed with 2% sodium dodecyl sulfate/7 M urea, and equal amounts of proteins from each sample were precipitated with acetone. Then, 50% trifluoroethanol and 4 mM dithiothreitol were added to denature and reduce the proteins, followed by alkylation of the free cysteine residues and trypsinization. The desalted peptides were then separated using liquid chromatography. The samples were subjected to LC–MS/MS (TripleTOF6600, AB Sciex, Tokyo, Japan) in the Scientific Research Facility Center, Hirosaki University Graduate School of Medicine. The mass spectrometer was operated in data-independent acquisition mode. A DIA-NN software version 1.8.1 extracted quantitative data for proteins from the data-independent acquisition (SWATH) using a library-free workflow. A predicted library

from a Swiss-Prot human database was built *in silico* with the options 'FASTA digest for library-free search/library generation' and 'Deep learning-based spectra, RTs and IMs prediction.' *H. pylori* proteins predicted from the genome information of the American Type Culture Collection and NCBI GenBank were used for *H. pylori* strains Tx30a (accession: f61942449fd6456f_1) and TN2wt (accession: AP019730.1), respectively. Quantitative data were output using RT-dependent cross-run normalization and filtering with a 1% FDR threshold. All other settings were left at their default values.

2.10 | Bioinformatics Analysis

The molecular weight and subcellular localization of each protein were predicted using Compute pI/Mw tool-ExPASY (https://web.expasy.org/compute_pi/) and PsortB v.3.0 (https://www.psort.org/psortb/), respectively. The STRING database (https://string-db.org/; v.12) was used for protein–protein interaction network (PPI) analysis. The interaction network generated using STRING was visualized in Cytoscape software (http://cytoscape.org/; v.3.10.1). The ClueGO plug-in of Cytoscape software was designed for the visualization and functional analysis of gene ontology (GO) terms and biological pathways. The GO annotates genes to biological/cellular/molecular terms in a hierarchical structure, while the Reactome pathways represent a comprehensive collection of molecular events and biological processes, including signaling pathways, metabolic pathways, and other cellular processes. In the selected proteins, GC-related proteins were selected using the *Homo sapiens* database.

2.11 | Statistical Analysis

Statistical analyses were performed using GraphPad Prism 9 software, and the method is mentioned in each figure legend. A p value < 0.05 is considered statistically significant.

3 | Results

3.1 | Isolations and Confirmation of EVs Derived From AGS Cells

H. pylori Tx30a is considered a low-virulence strain due to the absence of several key virulence factors that help *H. pylori* colonize and persist in the host stomach. The proteins identified in *H. pylori* Tx30a are available on the ATCC website (https://www.atcc.org/products/51932). BabA and SabA proteins, which play a role in the adhesion process, were absent in *H. pylori* Tx30a. Additionally, the virulence proteins such as CagPAI, OipA, DupA, and IceA commonly found in highly pathogenic strains that cause severe gastric diseases were also not present in *H. pylori* Tx30a. We conducted a cell infection experiment in which AGS cells were infected with these two strains and non-infected *H. pylori* (NI) for 48 h. A cytotoxic assay revealed a significant decrease in AGS cell viability when the cells were infected with either *H. pylori* strain. In addition, the cell viability of AGS cells infected with the low-virulence *H. pylori* strain was higher than that of the cells infected with the high-virulence strain (Figure S1). Therefore, in this study, the *H. pylori* Tx30a and *H. pylori* TN2wt were used to represent the low- and high-virulence *H. pylori* strains, respectively. AGS cells were infected with these two strains as well as a non-infected *H. pylori* (NI) for 48 h. The culture supernatant was then collected, and the EVs were isolated by ultracentrifugation (Figure 1, as the experimental workflow).

As mycoplasma infection could affect the constituents packaged into EVs, the absence of mycoplasma contamination was confirmed by PCR (Appendix S1). As shown in Additional Figure 1, our results provide evidence of the absence of mycoplasma contamination in the AGS cells. The triplicate-isolated EV samples derived from AGS cells with non-infection (AGSEVs-NI), *H. pylori* Tx30a (AGSEVs-Tx30a) infection, and *H. pylori* TN2wt (AGSEVs-TN2wt) infection were detected by immunoblotting analysis using the TSG101 antibody, a specific protein marker for EVs (Figure 2A). The isolated EVs derived from AGS cells were spherical in shape, 50 to 500 nm in diameter, and free from bacterial and cell debris, checked by negative-staining transmission electron microscopy (Figure 2B). This confirmed that our method isolated EVs as expected.

3.2 | Differential Proteomic Analysis of AGS Cells Infected With *H. pylori*

To investigate the differential expression of proteins (DEPs) in EVs derived from AGS cells infected with low- and high-virulence *H. pylori*. Using the EVs isolated from the AGS cells infected with *H. pylori* strains for 48 h, all the proteins were identified by LC–MS/MS.

A total of 2348 proteins were identified from AGSEVs-Tx30a and AGSEVs-NI. The group of 107 DEPs with significant differences was highly interconnected, as shown by STRING analysis (Figure S2A, Table S1). The most represented gene ontologies (GO) among these 107 DEPs were separately shown in terms of biological process (BP), molecular function (MF), and cellular component (CC), as shown in Figure S2B. In BP, the DEPs were highly involved in vacuolar transport, intracellular transport, establishment of localization in the cell, vesicle-mediated transport, and cellular localization, which play a crucial role in the functioning and organization of cells. To study the functional enrichment of the differential expression genes (DEGs) from the dataset, the Cytoscape plugin Cluego/CluePedia was used. The BP, MF, and CC of DEGs from the top five of the complex protein–protein interaction (PPI) networks were predominantly enriched in the dense body (GO:0097433), regulation of focal adhesion assembly (GO:0051893), structural constituent of cytoskeleton (GO:0005200), aminoacyl-tRNA synthetase multienzyme complex (GO:0017101) and vacuolar transport (GO:0007034) shown in Figure 3A. The REACTOME pathway analysis from ClueGO showed that many DEGs were significantly enriched in RHO GTPase effectors (R-HAS-195258), HCMV early events (R-HAS-9609690), tRNA aminoacylation (R-HSA-379724), Signaling by BRAF and RAF 1 fusion (R-HSA-6802952), RHO BTB GTPase cycle (R-HSA-97006574), and so forth as shown in Figure 3B.

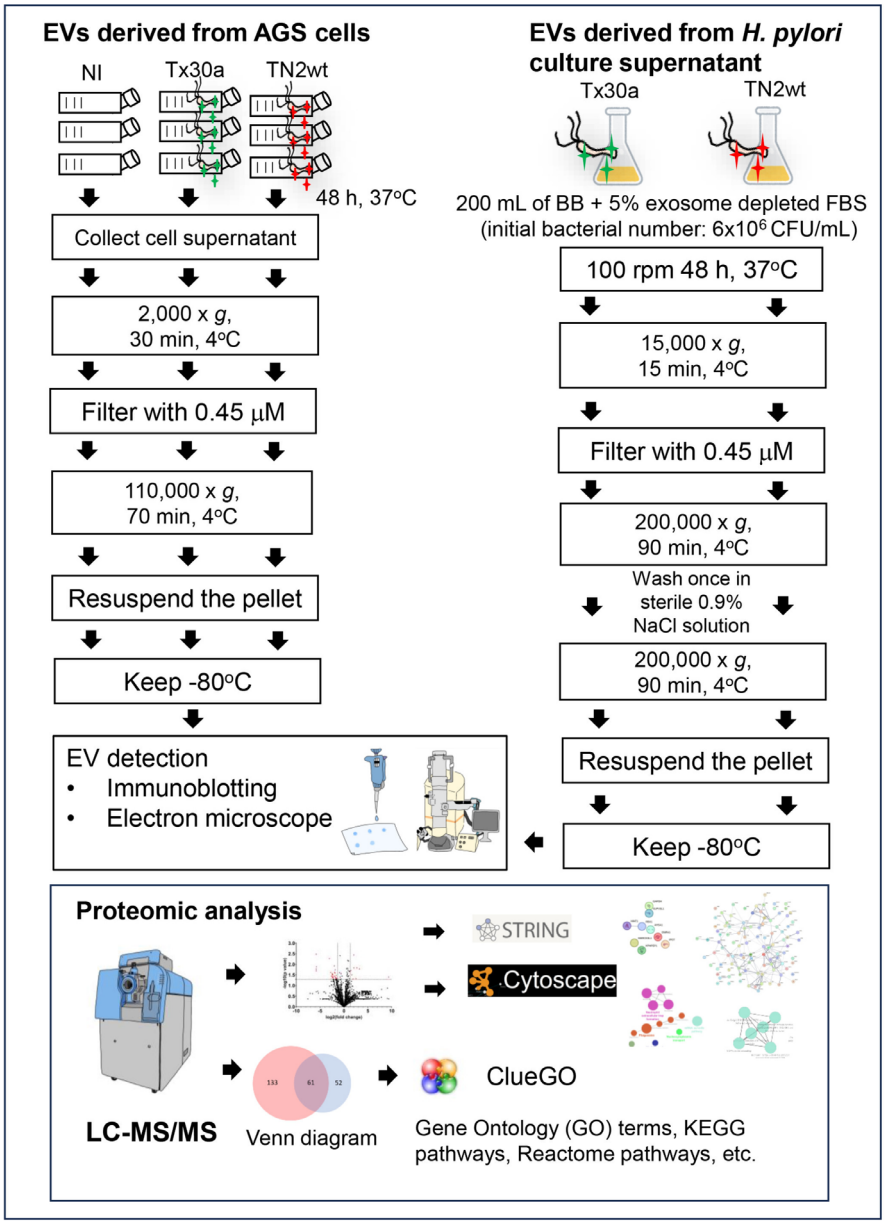

FIGURE 1 | Overview of the experiment flow and proteomic analysis by bioinformatic methods. NI, Non-infection with *H. pylori*.

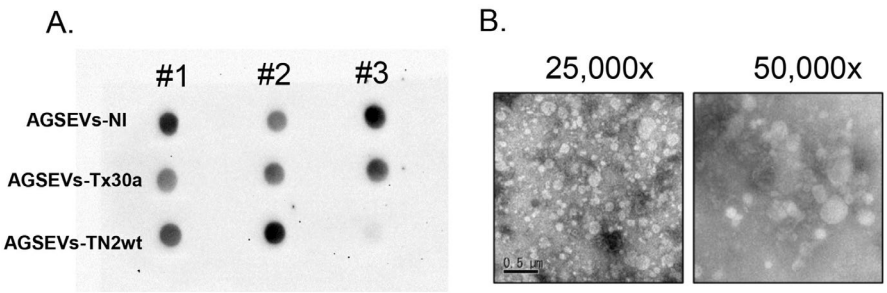

FIGURE 2 | The detection of AGS cell-derived EVs (AGSEVs). (A) Immunoblotting analysis using TSG101 antibody to dot blots of AGSEVs from non-infected cells (AGSEVs-NI), cells infected with *H. pylori* Tx30a (AGSEVs-Tx30a), and cells infected with *H. pylori* TN2wt (AGSEVs-TN2wt). (B) Negative staining of AGSEVs under electron microscopy. Scale bars: 500 nm; magnifications: 25,000× and 50,000×.

DEPs in AGSEVs-TN2wt and AGSEVs-NI were 2389 proteins. The group of 55 significantly different proteins was analyzed using STRING, as described above (Figure S3A, Table S2). The cellular components by GOs were azurophil granule lumen, extracellular exosome, extracellular space, vesicle, and extracellular region (Figure S3B). The function enrichment of DEGs

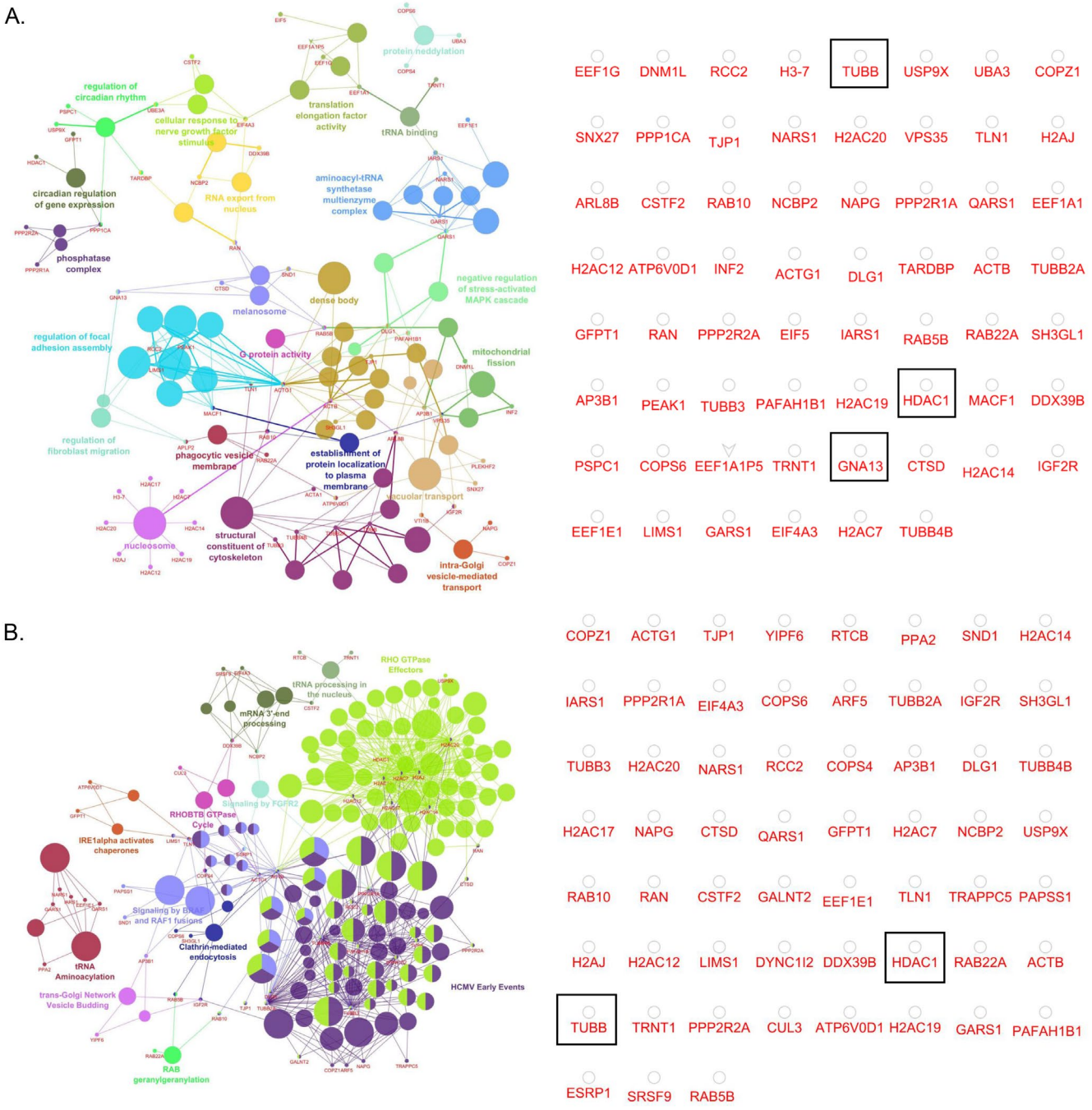

FIGURE 3 | Enrichment by Gene Ontology (GO) and pathway terms were visualized using the ClueGO/CluePedia plugin from Cytoscape. (A) The biological process (BP), molecular function (MF), and cellular component (CC) of DEGs PPI network of AGSEVs-Tx30a and AGSEVs-NI are shown. (B) The REACTOME pathway. The enrichment shows only significant GO terms and pathways ($p < 0.05$). The node color indicates the specific functional class that they are involved in. The colors represent various BP, MF, CC, and molecular pathways involved in the enrichment analysis of identified DEGs. The bold fonts indicate the most important functional GO terms and name of signaling pathway of each group. The names of the DEGs involved in each group are displayed in red font. The DEGs related to gastric cancer were shown in the black block.

from the dataset based on ClueGO revealed that the azurophil granule lumen (GO:0035578), purine nucleotide catabolic process (GO:0006195), ATPase-coupled cation transmembrane transport activity (GO:0019829), regulation of cellular response to insulin stimulus (GO:1900076), and killing of cells of another organism (GO:0031640) were predominant (Figure 4A). The REACTOME pathway analysis from ClueGO showed that many DEGs were significantly enriched in the regulation of RUNX2 expression and activity (R-HSA-8939902), E3 ubiquitin ligases ubiquitinate target proteins (R-HSA-8866654), iron uptake and transport (R-HSA-917937), and sensory processing of sound by inner hair cells of the cochlea (R-HSA-9662360) (Figure 4B).

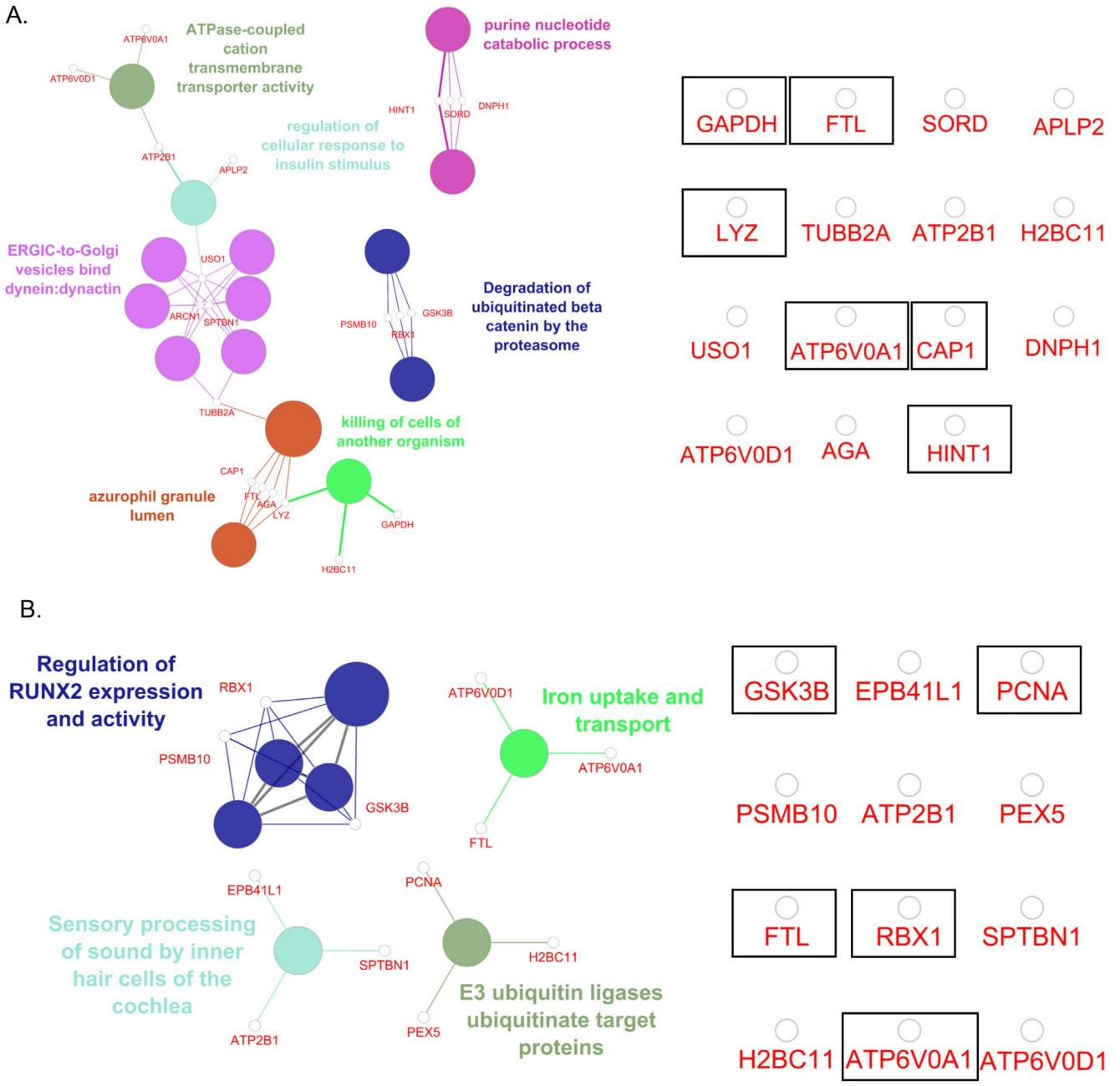

FIGURE 4 | Enrichment by Gene Ontology (GO) and pathway terms were visualized using the ClueGO/CluePedia plugin from Cytoscape. (A) The biological process (BP), molecular function (MF), and cellular component (CC) of DEGs PPI network of AGSEVs-TN2wt and AGSEVs-NI are shown. (B) The REACTOME pathway. The enrichment shows only significant GO terms and pathways ($p < 0.05$). The node color indicates the specific functional class that they are involved in. The colors represent various BP, MF, CC, and molecular pathways involved in the enrichment analysis of identified DEGs. The bold fonts indicate the most important functional GO terms and name of signaling pathway of each group. The names of the DEGs involved in each group are displayed in red font. The DEGs related to gastric cancer were shown in the black block.

3.3 | Potential of Candidate Markers

Over the past decades, many studies have proposed protein markers for diagnosing gastrointestinal cancers including GC, hepatocellular carcinoma (HCC), and colorectal cancer. Proteins such as ATP6V01, CAP1, FTL, GAPDH, GNA13, GSK3β, HDAC1, HINT1, PCNA, RBX1, and TUBB have been associated with GC, while LYZ has been linked to HCC [31–41]. GNA13 functions as an oncoprotein during GC progression by promoting G1/S cell cycle transition [34]. The activation of GSK3β is associated with cell proliferation, differentiation, and survival [35]. GSK3β plays a role in the Wnt signaling pathway in GC (KEGG pathway: hsa05226). In addition, RBX1 has been suggested to regulate cancer cell growth and survival [39].

Regarding the enrichments by GO terms and REACTOME pathway of DEGs PPI network (AGSEVs-Tx30a vs. AGSEVs-NI, AGSEVs-TN2wt vs. AGSEVs-NI), the DEGs that are related to GC were highlighted. ATP6V01, CAP1, FTL, GAPDH, GNA13, GSK3β, HDAC1, HINT1, LYZ, PCNA, RBX1, and TUBB were

found as GC-related DEGs, as shown in Figures 3 and 4 (red letter with black box at the right in both of figures). Interestingly, we found nine DEGs from AGSEVs-TN2wt that are related to GC (ATP6V0A1, CAP1, FTL, GAPDH, GSK3β, HINT1, LYZ, PCNA, and RBX1), while the DEGs from AGSEV-Tx30a included only three DEGs (GNA13, HDAC1, TUBB). This suggests that AGS cells infected with virulent *H. pylori* TN2wt are related to GC more than those AGS cells infected with non-virulent *H. pylori* Tx30a.

The volcano plot of DEPs between AGSEVs-Tx30a and AGSEVs-NI using a fold change cutoff of 2, log2FC > 1.3 or log2FC < −1.3 and FDR < 0.05 was shown in Figure 5A. Unsupervised hierarchical clustering analysis revealed that 48 proteins were upregulated, and five proteins were downregulated in AGSEVs-Tx30a compared to AGSEVs-NI. The PPI network of DEPs was performed by STRING analysis (Figure 5B, Table 1); there was only upregulated HDAC1 that reached statistical significance (Figure 5B; blue box,

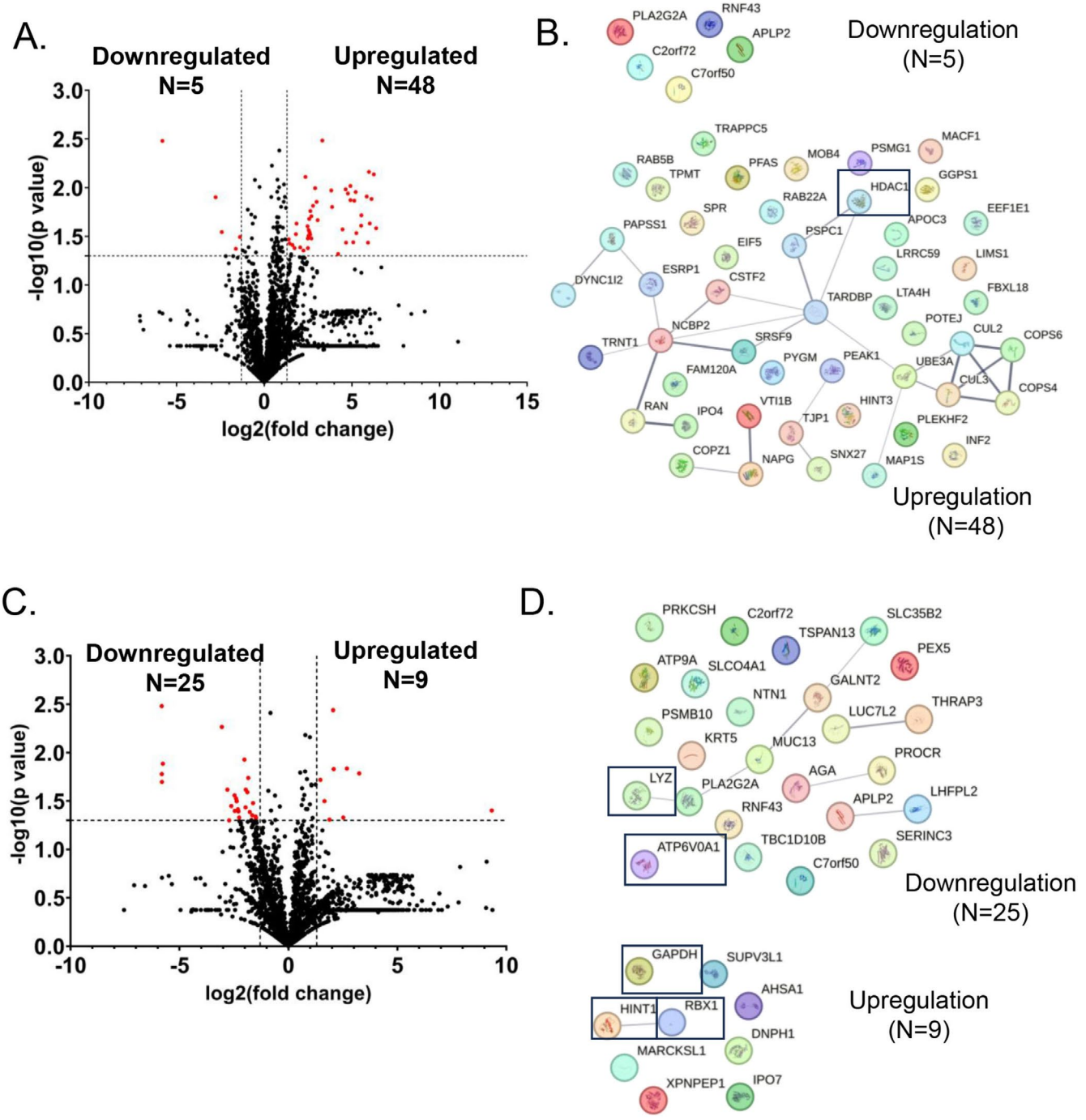

FIGURE 5 | Volcano plot of differential protein expression (DEPs) and protein–protein interaction (PPI) network of DEPs analyzed by STRING. (A) Volcano plot of DEPs between AGSEVs-Tx30a and AGSEVs-NI. (B) PPI network of DEPs between AGSEVs-Tx30a and AGSEVs-NI. (C) Volcano plot of DEPs between AGSEVs-TN2wt and AGSEVs-NI. (D) PPI network of DEPs between AGSEVs-TN2wt and AGSEVs-NI. Volcano plot: Black dots represented proteins that did not show significantly differential expression, while the red dots indicated the proteins with significantly differential expression. Cut-off: Log2FC > 1.3 or log2FC < −1.3 and FDR < 0.05.

TABLE 1 | The upregulated/downregulated DEPs between AGSEVs-Tx30a group and AGSEVs-NI group.

No.	Genes	Proteins	AGSEV-NI	AGSEVs-Tx30a	FC	Up/Downregulation
1	SPR	Sepiapterin reductase	0.41	4.11	3.32	Up
2	RNF43	E3 ubiquitin-protein ligase RNF43	5.63	0.10	−5.81	Down
3	CUL2	Cullin-2	0.10	6.29	5.98	Up
4	SRSF9	Serine/arginine-rich splicing factor 9	0.10	7.63	6.25	Up
5	POTEJ	POTE ankyrin domain family member J	19.30	98.45	2.35	Up
6	PSMG1	Proteasome assembly chaperone 1	0.10	3.03	4.92	Up
7	TJP1	Tight junction protein ZO-1	0.83	6.20	2.90	Up
8	MACF1	Microtubule-Actin cross-linking factor 1, isoforms 6/7	0.10	2.51	4.65	Up
9	NAPG	Gamma-soluble NSF attachment protein	0.75	10.63	3.83	Up
10	COPS6	COP9 signalosome complex subunit 6	0.10	3.72	5.22	Up
11	FAM120A	Constitutive coactivator of PPAR-gamma-like protein 1	0.10	2.74	4.78	Up
12	APOC3	Apolipoprotein C-III	0.10	5.77	5.85	Up
13	C2orf72	Uncharacterized protein C2orf72	5.62	0.82	−2.77	Down
14	DYNC1I2	Cytoplasmic dynein 1 intermediate chain 2	0.10	6.98	6.12	Up
15	GGPS1	Geranylgeranyl pyrophosphate synthase	0.10	3.03	4.92	Up
16	UBE3A	Ubiquitin-protein ligase E3A	0.10	3.52	5.14	Up
17	MOB4	MOB-like protein phocein	0.73	5.80	2.99	Up
18	PFAS	Phosphoribosylformylglycinamidine synthase	0.58	3.99	2.78	Up
19	COPZ1	Coatomer subunit zeta-1	0.71	10.31	3.87	Up
20	CUL3	Cullin-3	0.90	5.56	2.63	Up
21	TRNT1	CCA tRNA nucleotidyltransferase 1, mitochondrial	0.10	4.67	5.54	Up
22	ESRP1	Epithelial splicing regulatory protein 1	0.51	3.29	2.69	Up
23	COPS4	COP9 signalosome complex subunit 4	0.86	5.10	2.57	Up
24	NCBP2	Nuclear cap-binding protein subunit 2	0.58	4.80	3.05	Up
25	TRAPPC5	Trafficking protein particle complex subunit 5	0.10	6.50	6.02	Up
26	PAPSS1	Bifunctional 3′-phosphoadenosine 5′-phosphosulfate synthase 1	3.86	13.84	1.84	Up
27	TPMT	Thiopurine S-methyltransferase	0.10	4.62	5.53	Up
28	FBXL18	F-box/LRR-repeat protein 18	0.77	4.30	2.47	Up
29	INF2	Inverted formin-2	0.10	8.35	6.38	Up
30	VTI1B	Vesicle transport through interaction with t-SNAREs homolog 1B	0.10	2.22	4.47	Up
31	HINT3	Adenosine 5′-monophosphoramidase HINT3	0.54	3.15	2.54	Up
32	C7orf50	Uncharacterized protein C7orf50	5.43	1.01	−2.42	Down

(Continues)

TABLE 1 | (Continued)

No.	Genes	Proteins	AGSEV-NI	AGSEVs-Tx30a	FC	Up/Downregulation
33	PEAK1	Inactive tyrosine-protein kinase PEAK1	0.66	3.95	2.59	Up
34	PLEKHF2	Pleckstrin homology domain-containing family F member 2	0.10	3.83	5.26	Up
35	LTA4H	Leukotriene A-4 hydrolase	3.57	12.50	1.81	Up
36	PSPC1	Paraspeckle component 1	0.58	3.58	2.62	Up
37	EIF5	Eukaryotic translation initiation factor 5	2.33	13.42	2.53	Up
38	PLA2G2A	Phospholipase A2, membrane associated	620.95	237.74	−1.39	Down
39	EEF1E1	Eukaryotic translation elongation factor 1 epsilon-1	1.19	6.68	2.49	Up
40	LIMS1	LIM and senescent cell antigen-like-containing domain protein 1	1.31	8.48	2.69	Up
41	EEF1A1; P5	Elongation factor 1-alpha 1	66.67	175.92	1.40	Up
42	IPO4	Importin-4	0.10	3.38	5.08	Up
43	LRRC59	Leucine-rich repeat-containing protein 59	0.10	2.55	4.67	Up
44	SNX27	Sorting nexin-27	0.10	6.05	5.92	Up
45	RAN	GTP-binding nuclear protein Ran	90.84	247.47	1.45	Up
46	**HDAC1**	**Histone deacetylase 1**	**1.03**	**3.16**	**1.61**	**Up**.
47	RAB22A	Ras-related protein Rab-22A	1.57	6.54	2.06	Up
48	PYGM	Glycogen phosphorylase, muscle form	1.63	5.40	1.73	Up
49	MAP1S	Microtubule-associated protein 1S	0.42	2.34	2.49	Up
50	APLP2	Amyloid beta precursor like protein 2	8.60	2.80	−1.62	Down
51	TARDBP	TAR DNA-binding protein 43	0.86	4.04	2.24	Up
52	CSTF2	Cleavage stimulation factor subunit 2	0.26	4.78	4.22	Up
53	RAB5B	Ras-related protein Rab-5B	1.41	4.09	1.54	Up

bold in Table 1). Based on the same cutoff criteria, the volcano plot of DEPs between AGSEVs-TN2wt and AGSEVs-NI was shown in Figure 5C. Nine proteins were upregulated, and 25 proteins were downregulated in AGSEVs-TN2wt compared to AGSEVs-NI (Figure 5D, Table 2); there were five DEPs that reached statistical significance (upregulated RBX1, GAPDH, HINT1, and downregulated ATP6V0A1, LYZ) (Figure 5D; blue box, bold in Table 2). In our bioinformatic analysis comparing AGSEVs-TN2wt and AGSEVs-NI, ATP6V0A1 and RBX1 showed the highest fold change in up-/downregulation among other DEPs, reaching statistical significance. Only HDAC1 reached statistical significance in the comparison of AGSEVs-Tx30a and AGSEVs-NI. Along with the bioinformatic analysis in this study, the downregulation of ATP6V0A1 in PBMCs from GC patients, and the high expression of RBX1 and HDAC1 in GC biopsy samples were reported [31, 36, 39]. Therefore, we propose ATP6V0A1, RBX1, and HDAC1 as GC-related candidate EV biomarkers for *H. pylori* infection.

3.4 | Proteomic Analysis of HpEVs

We analyzed specific human proteins in EVs from cells infected with *H. pylori* and are also interested in what types of *H. pylori* proteins are delivered to EVs from *H. pylori* single culture (HpEVs) or dual culture as infection to AGS cells (AHpEVs). In this study, we isolated HpEVs from the culture supernatant of *H. pylori* Tx30a and TN2wt at 48 h of incubation. The growth curve of these two *H. pylori* strains is shown in Figure S4A. At 48 h of incubation, both bacterial strains were in the late exponential phase of the growth curve, and no significant differences were observed. Similarly, the viable bacterial counts at 48 h did not differ between the two *H. pylori* strains (Figure S4B). The viability of *H. pylori* cells was also observed using the LIVE/DEAD BacLight Bacterial Viability Kit. As shown in Figure S4C,D, the proportion of live (green) to dead (red; indicated by white arrows) cells at 48 h of incubation was not different between the Tx30a and TN2wt strains. Additionally, *H. pylori* cells at 48 h were bacilli, as shown in the enlarged figures in Figure S4C,D.

TABLE 2 | The upregulated/downregulated DEPs between the AGSEVs-TN2wt group and the AGSEVs-NI group.

No.	Genes	Proteins	AGSEV-NI	AGSEVs-TN2wt	FC	Up/Downregulation
1	RNF43	E3 ubiquitin-protein ligase RNF43	5.63	0.10	−5.81	Down
2	MARCKSL1	MARCKS-related protein	7.34	30.42	2.05	Up
3	PROCR	Endothelial protein C receptor	21.89	2.63	−3.06	Down
4	SLC35B2	Adenosine 3′-phospho 5′-phosphosulfate transporter 1	8.68	2.14	−2.02	Down
5	C7orf50	Uncharacterized protein C7orf50	5.43	0.10	−5.76	Down
6	AHSA1	Activator of 90 kDa heat shock protein ATPase homolog 1	1.65	10.61	2.69	Up
7	**HINT1**	**Adenosine 5′-monophosphoramidase HINT1**	**6.82**	**28.82**	**2.08**	**Up**
8	**RBX1**	**E3 ubiquitin-protein ligase RBX1**	**0.90**	**8.59**	**3.25**	**Up**
9	C2orf72	Uncharacterized protein C2orf72	5.62	0.10	−5.81	Down
10	PEX5	Peroxisomal targeting signal 1 receptor	15.97	4.46	−1.84	Down
11	**GAPDH**	**Glyceraldehyde-3-phosphate dehydrogenase**	**258.69**	**715.84**	**1.47**	**Up**
12	AGA	N(4)-(beta-N-acetylglucosaminyl)-L-asparaginase	5.59	0.10	−5.80	Down
13	TBC1D10B	TBC1 domain family member 10B	6.54	1.68	−1.96	Down
14	**ATP6V0A1**	**V-type proton ATPase 116 kDa subunit a 1**	**7.12**	**1.02**	**−2.80**	**Down**
15	KRT5	Keratin, type II cytoskeletal 5	7.22	1.96	−1.88	Down
16	MUC13	Mucin-13	7.24	1.30	−2.47	Down
17	NTN1	Netrin-1	8.75	1.65	−2.40	Down
18	LHFPL2	LHFPL tetraspan subfamily member 2 protein	2.97	0.57	−2.38	Down
19	XPNPEP1	Xaa-Pro aminopeptidase 1	3.28	10.33	1.66	Up
20	GALNT2	Polypeptide N-acetylgalactosaminyltransferase 2	13.83	2.67	−2.37	Down
21	**LYZ**	**Lysozyme C**	**743.58**	**241.53**	**−1.62**	**Down**
22	PRKCSH	Glucosidase 2 subunit beta	6.50	1.05	−2.62	Down
23	THRAP3	Thyroid hormone receptor-associated protein 3	7.91	2.02	−1.97	Down
24	APLP2	Amyloid beta precursor like protein 2	8.60	1.73	−2.32	Down
25	SUPV3L1	ATP-dependent RNA helicase SUPV3L1, mitochondrial	0.10	64.54	9.33	Up
26	TSPAN13	Tetraspanin-13	7.66	1.39	−2.47	Down
27	LUC7L2	Putative RNA-binding protein Luc7-like 2	16.84	3.42	−2.30	Down
28	SERINC3	Serine incorporator 3	7.10	2.07	−1.78	Down
29	SLCO4A1	Solute carrier organic anion transporter family member 4A1	13.53	4.29	−1.66	Down

(Continues)

TABLE 2 | (Continued)

No.	Genes	Proteins	AGSEV-NI	AGSEVs-TN2wt	FC	Up/Downregulation
30	ATP9A	Probable phospholipid-transporting ATPase IIA	13.28	4.67	−1.51	Down
31	DNPH1	2′-deoxynucleoside 5′-phosphate N-hydrolase 1	2.20	12.61	2.52	Up
32	PSMB10	Proteasome subunit beta type-10	5.03	1.05	−2.26	Down
33	PLA2G2A	Phospholipase A2, membrane associated	620.95	221.34	−1.49	Down
34	IPO7	Importin-7	4.88	17.98	1.88	Up

Note: DEPs that reached stastical significance are highlighted in bold.

At first, HpEVs were isolated in triplicate from the culture supernatant of *H. pylori* Tx30a and TN2wt by ultracentrifugation. The HpEVs-Tx30a and HpEVs-TN2wt protein profiles were identified by using LC–MS/MS. One hundred and eight and 194 proteins were detected in HpEVs-Tx30a and HpEVs-TN2wt (Tables S3 and S4). There was an overlap in the essential proteins identified for *H. pylori* survival and virulence. For example, the major outer membrane family includes outer membrane proteins Hop, Hof, Hor, and Hom families, iron-regulated outer membrane proteins (FrpB), and iron (III) dicitrate transport protein (FecA). Proteins related to cell wall and membrane biogenesis include membrane fusion protein (MtrC), rare lipoprotein A (RlpA), and protease. Cell motility-related proteins include flagellin A, flagellin B, flagella hook-associated proteins (FlgE, FlgL, FlgK), flagellar basal body rod modified protein (FlgD), and flagella sheath adhesin (HpaA). Metabolism-related proteins include ATP-dependent nuclease (AddB), amino acid ABC transporter substrate-binding protein, ABC transporter glutamine-binding protein (GlnH), ATP synthase subunits alpha and beta (AtpA, AtpD), cytochrome c553 (Cytc553), nuclease NucT, 2′,3′-cyclic-nucleotide 2′-phosphodiesterase (CpdB) and iron (III) ABC transport periplasmic iron-binding protein (CeuE). Post-translation modification-related proteins include chaperone and heat shock protein (GroEL), 60 kDa chaperone (GroL), co-chaperone (GroES), and bifunctional methionine sulfoxide reductase A/B (MsrA). *H. pylori* virulence-related proteins include urease subunits alpha and beta (UreA, UreB), VacA, CagPAI, and CagA. In addition, we detected BabA adhesin, the important protein for adherence, and delivery of other effector molecules by *H. pylori* to host cells.

3.5 | Differential Proteomic Analysis of HpEVs Tx30a, TN2wt and Compare With Those Derived From AGS Infection

H. pylori produces different proteins during growth in culture medium compared to during host cell infection. One of our objectives was to search for *H. pylori* protein markers that represent highly virulent *H. pylori* infection. We are interested in the proteins that highly virulent *H. pylori* strains express during cell infection. To investigate the HpEVs protein profiles of HpEVs derived from bacteria culture supernatant (BCS) and HpEVs/proteins derived from *H. pylori*-infected AGS cell culture supernatant (CCS), the proteomic analysis was performed. There were 99 common proteins in the two groups investigated (HpEVs-Tx30a; from BCS vs. AHpEVs-Tx30a; from CCS) as described in the Venn diagram (Figure 6A, Table S3). There were 61 common proteins in HpEVs-TN2wt from BCS vs. AHpEVs-TN2wt from CCS as indicated in Figure 6B and Table S4. *H. pylori* produces distinct protein profiles depending on its environment. During AGS cell infection, *H. pylori* mainly expresses proteins related to adhesins, toxins, and secretion system components that are critical for colonization, virulence, and immune modulation. In contrast, proteins produced during growth in culture media are mainly involved in metabolism, cell replication, and some virulence functions. However, certain *H. pylori* proteins are expressed under both conditions. There were 52 proteins that *H. pylori* TN2wt expressed during infection to AGS cells (Table S5) and only 15 *H. pylori* proteins exist in AHpEVs-TN2wt-infected AGS cells, but not in AHpEVs-Tx30a-infected AGS cells (bold in Figure 6C). These proteins are related to enzymes in metabolic pathways, lipopolysaccharide biosynthesis, flagella assembly, and more. The proteins involved in the metabolism are N-methylhydantoinase, proline peptidase, glutamine synthetase, NADH dehydrogenase subunit B, and Thioesterase. Neutrophil-activating protein A is involved in the immune response and activates neutrophils. Alkyl hydroperoxide reductase/thiol-specific antioxidant/Mal allergen and more are involved in the oxidative stress response. These EV proteins are of interest in their special function in helping *H. pylori* to survive in the stomach (bold in Table S5).

Many studies have reported that *H. pylori* CagA is associated with GC; the unknown factors other than CagA also contribute to GC development and immune invasion [42–44]. *H. pylori* peptidoglycan is recognized by NOD1, an intracellular pathogen recognition receptor, leading to a pro-inflammatory response through an NF-κB dependent pathway [45]. In addition, NF-κB dependent expression of the DNA editing enzyme, activation-induced cytidine deaminase (AID), in host cells results in the accumulation of mutations in the tumor suppressor protein TP53. The induction of AID may represent a mechanism by which gene mutations arise during *H. pylori*-associated gastric carcinogenesis [46]. Regarding this mechanism, the unknown proteins from *H. pylori* could act as carcinogens and contribute to gastric carcinogenesis.

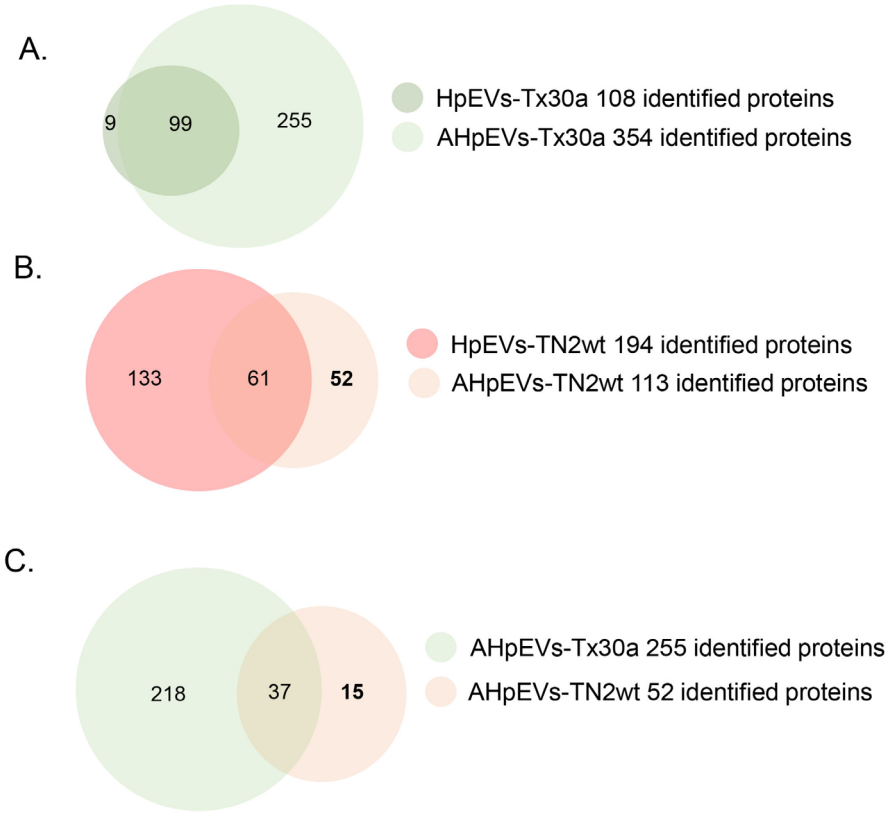

FIGURE 6 | Venn diagram of proteomic analysis of HpEVs. The Venn diagram displays the proteomic analysis of HpEVs derived from bacteria culture supernatant (HpEVs) and from *H. pylori*-infected AGS cell culture supernatant (AHpEVs). (A) HpEV-Tx30a and AHpEVs-Tx30a. (B) HpEVs-TN2wt and AHpEVs-TN2wt. (C) AHpEVs-Tx30a and AHpEVs-TN2wt. Identified proteins from AHpEVs-TN2wt were listed in Table S5.

4 | Discussion

Blood-based biomarkers have been developed to minimize invasive techniques, particularly in the diagnosis of cancers and infectious diseases [20, 21]. Unfortunately, this technology for screening the markers of *H. pylori* infection, especially caused by the virulence strain, is still unknown. We aimed to identify the candidate protein markers for detecting virulent *H. pylori* infections in EVs derived from gastric cell lines, which could be developed for the detection of body fluids in the future. Nine GC-related proteins were observed in EVs derived from highly virulent *H. pylori* TN2wt-infected AGS cells (ATP6V0A1, CAP1, FTL, GAPDH, GSK3β, HINT1, LYZ, PCNA, and RBX1), whereas only three proteins were detected in EVs derived from low-virulent *H. pylori* Tx30a-infected AGS cells (GNA13, HDAC1, TUBB). The difference between these two strains is that *H. pylori* TN2wt is CagA-positive, *vacA* s1m1 type, while *H. pylori* Tx30a has CagA-negative, *vacA* s2m2 type. CagA-positive and *vacA* s1m1 *H. pylori* strains increase the risk of GC compared to CagA-negative and *vacA* s2m2 strains [6, 8, 47]. Other virulence factors associated with severe outcomes in the patient, such as BabA, SabA, OipA, DupA, and IceA, were not found in the low-virulence *H. pylori* Tx30a. Therefore, nine GC-related proteins from virulent *H. pylori-infected* cells, and even three GC-related proteins from non-virulent *H. pylori-infected* cells, were 12 potential candidate proteins to screen GC-related *H. pylori* infection from EVs in blood samples.

Based on a fold change cutoff of 2, $\log2FC > 1.3$ or $\log2FC < -1.3$ and FDR < 0.05, five DEPs were found to be significantly different between AGSEVs-TN2wt and AGSEVs-NI (ATP6V0A1, GAPDH, HINT1, LYZ, and RBX1), whereas only HDAC1 was found to be significantly different between AGSEVs-Tx30a and AGSEVs-NI. Based on bioinformatics analysis and research reports, ATP6V0A1, RBX1, and HDAC1 were chosen as the candidate proteins. It has been reported that ATP6V0A1, GAPDH, and Hint1 are downregulated in the GC tissue [31, 37] while LYZ, RBX1, and HDAC1 are up-regulated in hepatocellular carcinoma and GC [36, 39, 41]. Gene expression in peripheral blood samples from GC patients and healthy volunteers by microarray analysis revealed that ATP6V0A1 was found to be downregulated in the GC tissue [31]. RBX1 could be used as the predictor for the postoperative survival of GC patients, as higher expression of RBX1 correlated significantly with worse postoperative overall survival [39]. Low HDAC1 expression was associated with better overall survival compared to high HDAC1 expression in gastrointestinal malignancy, suggesting that HDAC1 could be a good diagnostic and prognostic marker [36].

HpEVs derived from *H. pylori* culture supernatants contain essential components, including nucleic acids, enzymes, proteins, toxins, and more, for their survival and pathogenicity [19]. We detected the majority of outer membrane proteins (Hop, Hof, Hor, and Hom), iron-regulated outer membrane proteins (FrpB and FecA), metabolism proteins (AddB, GlnH, AtpA, AtpD, Cytc553, and CeuE), and post-translation and modification-related proteins (GroEL, GroES, GroL, and MsrA) in the HpEVs. The *H. pylori* proteins related to host cell infection (BabA adhesin and flagellins) and virulence-related proteins (UreA, UreB, VacA and CagA). A study revealed that BabA, SabA, and oncoprotein CagA are important effectors in disease development [48]. Fewer and less

diverse *H. pylori* proteins were found in small HpEVs compared to larger HpEVs. Larger HpEVs contained many of the adhesins, iron-regulated proteins, the Hop family of outer membrane proteins, BabA, flagella basal, and hook proteins, while the small HpEVs were associated with metabolism-related proteins, glutamine synthetase, flavodoxin, type II citrate synthase, and non-heme iron-containing ferritin [19]. Our results showed differences in protein profiles of HpEVs derived from BCS versus those derived from CCS (Tables S3 and S4). This suggests that environmental conditions affect the protein contents in HpEVs.

Considering the potential of EVs derived from host cells or *H. pylori* to be used as the liquid-based biomarker for the diagnosis of *H. pylori* infection and *H. pylori*-caused GC, these markers are useful for screening, particularly in areas with a high incidence of GC. Based on our study, it is clear that high- and low-virulence *H. pylori* affect host cell proteins in EVs differently. Additionally, *H. pylori* produces different protein compositions in HpEVs based on environmental conditions. For further study, we plan to use the *H. pylori* clinical isolates in the experiments and validate these candidate proteins (ATP6V0A1, RBX1, and HDAC1) in patient serum to address our limitations.

5 | Conclusions

In this study, we characterized the protein profile of EVs derived from AGS cells infected with different types of *H. pylori*. We observed several GC-related host proteins in EVs from AGS cells infected with a high-virulence *H. pylori* strain. In addition, the *H. pylori* proteins in HpEVs derived from bacterial culture supernatant and *H. pylori*-infected AGS cell culture supernatant were identified. Either the candidate proteins in EVs from host cells or *H. pylori* can be used as the liquid-based biomarker for screening the *H. pylori* infection, resulting in a decrease in GC cases reported in the future, particularly the *H. pylori* infection-related GC.

Author Contributions

Phawinee Subsomwong: conceptualization, data curation, formal analysis, investigation, methodology, writing – original, writing – review and editing, funding acquisition, project administration. **Krisana Asano:** supervision, validation, methodology, writing – review and editing, funding acquisition. **Junko Akada:** validation, methodology. **Takashi Matsumoto:** validation, methodology. **Akio Nakane:** validation, writing – review and editing, funding acquisition. **Yoshio Yamaoka:** resources, funding acquisition, supervision, validation, writing – review and editing.

Acknowledgments

The authors gratefully thank the Scientific Research Facility Center, Hirosaki University Graduate School of Medicine, for the differential proteomic analysis.

Ethics Statement

The authors have nothing to report.

Conflicts of Interest

The authors declare no conflicts of interest.

Data Availability Statement

The proteomic data of AGSEVs-NI, AGSEVs-Tx30a, and AGSEVs-TN2wt are available under accession number PXD056529 and JPST003403 for Proteome Xchange and jPOST Repository, respectively. The identification proteins of HpEVs *H. pylori* Tx30a and *H. pylori* TN2wt are available under accession numbers PXD056530, JPST003407 and PXD056531, JPST003408, respectively.

References

1. J. K. Y. Hooi, W. Y. Lai, W. K. Ng, et al., "Global Prevalence of *Helicobacter pylori* Infection: Systematic Review and Meta-Analysis," *Gastroenterology* 153, no. 2 (2017): 420–429.

2. S. Suerbaum and P. Michetti, "*Helicobacter pylori* Infection," *New England Journal of Medicine* 347, no. 15 (2002): 1175–1186.

3. R. M. Peek and M. J. Blaser, "*Helicobacter pylori* and Gastrointestinal Tract Adenocarcinomas," *Nature Reviews Cancer* 2, no. 1 (2002): 28–37.

4. F. Bray, M. Laversanne, H. Sung, et al., "Global Cancer Statistics 2022: GLOBOCAN Estimates of Incidence and Mortality Worldwide for 36 Cancers in 185 Countries," *CA: A Cancer Journal for Clinicians* 74, no. 3 (2024): 229–263.

5. P. Correa, "Human Gastric Carcinogenesis: A Multistep and Multifactorial Process-First American Cancer Society Award Lecture on Cancer Epidemiology and Prevention," *Cancer Research* 52, no. 24 (1992): 6735–6740.

6. M. J. Blaser, G. I. Perez-Perez, H. Kleanthous, et al., "Infection With *Helicobacter pylori* Strains Possessing *cagA* Is Associated With an Increased Risk of Developing Adenocarcinoma of the Stomach," *Cancer Research* 55, no. 10 (1995): 2111–2115.

7. L. J. van Doorn, C. Figueiredo, R. Sanna, et al., "Clinical Relevance of the *cagA*, *vacA*, and *iceA* Status of *Helicobacter pylori*," *Gastroenterology* 115, no. 1 (1998): 58–66.

8. J. L. Rhead, D. P. Letley, M. Mohammadi, et al., "A New *Helicobacter pylori* Vacuolating Cytotoxin Determinant, the Intermediate Region, Is Associated With Gastric Cancer," *Gastroenterology* 133, no. 3 (2007): 926–936.

9. M. Sugimoto, M. R. Zali, and Y. Yamaoka, "The Association of *vacA* Genotypes and *Helicobacter pylori*-Related Gastroduodenal Diseases in the Middle East," *European Journal of Clinical Microbiology and Infectious Diseases* 28, no. 10 (2009): 1227–1236.

10. D. Doohan, Y. A. A. Rezkitha, L. A. Waskito, Y. Yamaoka Y, and M. Miftahussurur, "*Helicobacter pylori* BabA-SabA Key Roles in the Adherence Phase: The Synergic Mechanism for Successful Colonization and Disease Development," *Toxins (Basel)* 13, no. 7 (2021): 485.

11. Y. Yamaoka, S. Kikuchi, H. M. T. el-Zimaity, O. Gutierrez, M. S. Osato, and D. Y. Graham, "Importance of Helicobacter pylori *oipA* in Clinical Presentation, Gastric Inflammation, and Mucosal Interleukin 8 Production," *Gastroenterology* 123, no. 2 (2002): 414–424.

12. S. W. Jung, M. Sugimoto, S. Shiota, D. Y. Graham, and Y. Yamaoka, "The Intact *dupA* Cluster Is a More Reliable *Helicobacter pylori* Virulence Marker Than *dupA* Alone," *Infection and Immunity* 80, no. 1 (2012): 381–387.

13. S. Shiota, M. Watada, O. Matsunari, S. Iwatani, R. Suzuki, and Y. Yamaoka, "Helicobacter pylori *iceA*, Clinical Outcomes, and Correlation With *cagA*: A Meta-Analysis," *PLoS One* 7, no. 1 (2012): e30354.

14. S. L. N. Maas, X. O. Breakefield, and A. M. Weaver, "Extracellular Vesicles: Unique Intercellular Delivery Vehicles," *Trends in Cell Biology* 27, no. 3 (2017): 172–188.

15. H. Bu, D. He, X. He, and K. Wang, "Exosomes: Isolation, Analysis, and Applications in Cancer Detection and Therapy," *Chembiochem: A European Journal of Chemical Biology* 20, no. 4 (2019): 451–461.

16. G. D. He, Y. Q. Huang, L. Liu, et al., "Association of Circulating, Inflammatory-Response Exosomal mRNAs With Acute Myocardial Infarction," *Frontiers in Cardiovascular Medicine* 8 (2021): 712061.

17. J. Nilsson, J. Skog, A. Nordstrand, et al., "Prostate Cancer-Derived Urine Exosomes: A Novel Approach to Biomarkers for Prostate Cancer," *British Journal of Cancer* 100, no. 10 (2009): 1603–1607.

18. M. E. Zahmatkesh, M. Jahanbakhsh, N. Hoseini, et al., "Effects of Exosomes Derived From *Helicobacter pylori* Outer Membrane Vesicle-Infected Hepatocytes on Hepatic Stellate Cell Activation and Liver Fibrosis Induction," *Frontiers in Cellular and Infection Microbiology* 12 (2022): 857570.

19. L. Turner, N. J. Bitto, D. L. Steer, et al., "*Helicobacter pylori* Outer Membrane Vesicle Size Determines Their Mechanisms of Host Cell Entry and Protein Content," *Frontiers in Immunology* 9 (2018): 1466.

20. J. P. Hinestrosa, R. Kurzrock, J. M. Lewis, et al., "Early-Stage Multi-Cancer Detection Using an Extracellular Vesicle Protein-Based Blood Test," *Communications Medicine* 2, no. 1 (2022): 29.

21. J. P. Hinestrosa, R. C. Sears, H. Dhani, et al., "Development of a Blood-Based Extracellular Vesicle Classifier for Detection of Early-Stage Pancreatic Ductal Adenocarcinoma," *Communications Medicine* 3, no. 1 (2023): 146.

22. R. Bandu, J. W. Oh, and K. P. Kim, "Extracellular Vesicle Proteins as Breast Cancer Biomarkers: Mass Spectrometry-Based Analysis," *Proteomics* 24, no. 11 (2024): e2300062.

23. F. Tian, S. Zhang, C. Liu, et al., "Protein Analysis of Extracellular Vesicles to Monitor and Predict Therapeutic Response in Metastatic Breast Cancer," *Nature Communications* 12, no. 1 (2021): 2536.

24. D. Huang, D. Rao, X. Xi, Z. Zhang, and T. Zhong, "Application of Extracellular Vesicles Proteins in Cancer Diagnosis," *Frontiers in Cell and Developmental Biology* 10 (2022): 1007360.

25. S. Akbar, A. Raza, R. Mohsin, et al., "Circulating Exosomal Immuno-Oncological Checkpoints and Cytokines Are Potential Biomarkers to Monitor Tumor Response to Anti-PD-1/PD-L1 Therapy in Non-Small Cell Lung Cancer Patients," *Frontiers in Immunology* 13 (2022): 1097117.

26. C. Gu, A. Shang, G. Liu, et al., "Identification of CD147-Positive Extracellular Vesicles as Novel Non-Invasive Biomarkers for the Diagnosis and Prognosis of Colorectal Cancer," *Clinica Chimica Acta* 548 (2023): 117510.

27. A. E. Ballok, L. M. Filkins, J. M. Bomberger, B. A. Stanton, and G. A. O'Toole, "Epoxide-Mediated Differential Packaging of Cif and Other Virulence Factors Into Outer Membrane Vesicles," *Journal of Bacteriology* 196, no. 20 (2014): 3633–3642.

28. A. Palacios, L. Sampedro, I. A. Sevilla, et al., "*Mycobacterium tuberculosis* Extracellular Vesicle-Associated Lipoprotein LpqH as a Potential Biomarker to Distinguish Paratuberculosis Infection or Vaccination From Tuberculosis Infection," *BMC Veterinary Research* 15, no. 1 (2019): 188.

29. J. Melo, V. Pinto, T. Fernandes, et al., "Isolation Method and Characterization of Outer Membranes Vesicles of *Helicobacter pylori* Grown in a Chemically Defined Medium," *Frontiers in Microbiology* 12 (2021): 654193.

30. P. Subsomwong, W. Teng, T. Ishiai, et al., "Extracellular Vesicles From *Staphylococcus aureus* Promote the Pathogenicity of *Pseudomonas aeruginosa*," *Microbiological Research* 281 (2024): 127612.

31. N. Matsumura, H. Zembutsu, K. Yamaguchi, et al., "Identification of Novel Molecular Markers for Detection of Gastric Cancer Cells in the Peripheral Blood Circulation Using Genome-Wide Microarray Analysis," *Experimental and Therapeutic Medicine* 2, no. 4 (2011): 705–713.

32. S. Xie, C. Shen, S. Zhou, et al., "Role of Adenylate Cyclase-Associated Protein 1 in Cancer," *International Journal of Clinical and Experimental Medicineis* 4 (2018): 30886–33099.

33. L. Zhang, Z. Chen, and A. Xu, "FTL: A Novel Predictor in Gastric Cancer," *International Journal of Clinical and Experimental Medicineis* 7 (2017): 7865–7872.

34. J. X. Zhang, M. Yun, Y. Xu, et al., "GNA13 as a Prognostic Factor and Mediator of Gastric Cancer Progression," *Oncotarget* 7, no. 4 (2016): 4414–4427.

35. Y. J. Cho, J. H. Kim, J. Yoon, et al., "Constitutive Activation of Glycogen Synthase Kinase-3 Beta Correlates With Better Prognosis and Cyclin-Dependent Kinase Inhibitors in Human Gastric Cancer," *BMC Gastroenterology* 10 (2010): 91.

36. L. L. Cao, Z. Yue, L. Liu, et al., "The Expression of Histone Deacetylase HDAC1 Correlates With the Progression and Prognosis of Gastrointestinal Malignancy," *Oncotarget* 8, no. 24 (2017): 39241–39253.

37. H. Huang, X. Wei, X. Su, et al., "Clinical Significance of Expression of Hint1 and Potential Epigenetic Mechanism in Gastric Cancer," *International Journal of Oncology* 38, no. 6 (2011): 1557–1564.

38. S. Yin, Z. Li, J. Huang, et al., "Prognostic Value and Clinicopathological Significance of Proliferating Cell Nuclear Antigen Expression in Gastric Cancer: A Systematic Review and Meta-Analysis," *Oncotargets and Therapy* 10 (2017): 319–327.

39. K. Migita, T. Takayama, S. Matsumoto, et al., "Prognostic Impact of RING Box Protein-1 (RBX1) Expression in Gastric Cancer," *Gastric Cancer* 17, no. 4 (2014): 601–609.

40. J. Yu, J. Goa, Z. Lu, Y. Li, and L. Shen, "Serum Levels of TUBB3 Correlate With Clinical Outcome in Chinese Patients With Advanced Gastric Cancer Receiving First-Line Paclitaxel Plus Capecitabine," *Medical Oncology* 29, no. 5 (2012): 3029–3034.

41. Z. Gu, L. Wang, Q. Dong, et al., "Aberrant LYZ Expression in Tumor Cells Serves as the Potential Biomarker and Target for HCC and Promotes Tumor Progression via csGRP78," *Proceedings of the National Academy of Sciences of the United States of America* 120, no. 29 (2023): e2215744120.

42. D. Y. Graham and Y. Yamaoka, "*H. Pylori* and *cagA*: Relationships With Gastric Cancer, Duodenal Ulcer, and Reflex Esophagitis and Its Complications," *Helicobacter* 3, no. 3 (1998): 145–151.

43. Z. W. Chen, Z. B. Dong, H. T. Xiang, S. S. Chen, W. M. Yu, and C. Liang, "*Helicobacter pylori* CagA Protein Induces Gastric Cancer Stem Cell-Like Properties Through the Akt/FOXO3 Axis," *Journal of Cellular Biochemistry* 125, no. 3 (2024): e30537.

44. N. Tegtmeyer, S. Wessler, and S. Backert, "Role of the Cag-Pathogenicity Island Encoded Type IV Secretion System in *Helicobacter pylori* Pathogenesis," *FEBS Journal* 279, no. 9 (2011): 1190–1202.

45. J. Viala, C. Chaput, I. G. Boneca, et al., "Nod1 Responds to Peptidoglycan Delivered by the *Helicobacter pylori* Cag Pathogenicity Island," *Nature Immunology* 5, no. 11 (2004): 1166–1174.

46. Y. Matsumoto, H. Marusawa, K. Kinoshita, et al., "*Helicobacter pylori* Infection Triggers Aberrant Expression of Activation-Induced Cytidine Deaminase in Gastric Epithelium," *Nature Medicine* 13, no. 4 (2007): 47–476.

47. J. Y. Park, D. Forman, L. A. Waskito, and Y. Yamaoka, "Epidemiology of *Helicobacter Pylori* and CagA-Positive Infections and Global Variations in Gastric Cancer," *Toxins (Basel)* 10, no. 4 (2018): 163.

48. A. Olofsson, A. Vallström, K. Petzold, et al., "Biochemical and Functional Characterization of *Helicobacter pylori* Vesicles," *Molecular Microbiology* 77, no. 6 (2010): 1539–1555.

Supporting Information

Additional supporting information can be found online in the Supporting Information section.